Anomalous retardation of relativistic plasmons: Microwave response of a gated two-dimensional electron system

A. M. Zarezin [1,2,*] V. M. Muravev,[1,*] P. A. Gusikhin,[1] A. A. Zabolotnykh [3] V. A. Volkov [3] and I. V. Kukushkin[1]

[1]*Institute of Solid State Physics, RAS, Chernogolovka, 142432 Russia*
[2]*Moscow Institute of Physics and Technology, Dolgoprudny, 141700 Russia*
[3]*Kotelnikov Institute of Radio-engineering and Electronics of the RAS, Mokhovaya 11-7, Moscow 125009, Russia*

We investigate the microwave response of a gated two-dimensional electron system (2DES) loaded by an external on-chip resonator. We find the system response to be dominated by the excitation of relativistic plasmons. These plasmons exhibit anomalously strong coupling to the photon mode of the resonator, which manifests itself in a drastic reduction of the plasma resonant frequency and linewidth. We develop an analytical approach to explain the observed phenomenon of strong interaction of 2D plasma with light. The theory turned out to be in good agreement with the experiment.

The interaction between light and matter is at the heart of nearly every optical process found in nature. It gives rise to hybrid light-matter modes, involving collective oscillations of polarization charges in matter—polaritons [1,2]. The most compelling feature of polaritons is that they trap light far below the optical wavelength [3,4]. As a result, an increase in the associated electric field strength leads to enhanced light-matter interaction. A prominent example is the most-studied case of surface plasmon polaritons supported by electrons in metals [5]. High-quality two-dimensional electron system (2DES) can support a new class of polaritons—2D plasmon polaritons [6–8]. Two-dimensional systems have been proven an ideal platform for studying polariton effects due to their high purity and wide parameter tunability [9–15].

Previous experiments have shown that a partly gated 2DES supports a new family of plasma waves, including relativistic plasmons [16–18] and proximity plasmons [19–22]. Relativistic plasmons are the electron density oscillations between the 2D electron subsystem and the gate over the 2DES [18]. The excitation of these plasma oscillations requires the gate to be electrically connected to the 2DES through an external circuit. Most importantly, it has been found that relativistic plasmons have anomalously weak damping due to strong interaction between the 2D plasma and the photon mode of the external resonator. For this reason, it is possible to observe relativistic plasmons even at $\omega_p \tau \ll 1$ (where ω_p is the plasmon frequency and τ is the momentum relaxation time of electrons), when ordinary 2D plasmons are overdamped.

Although the physical origin of relativistic plasma excitations has recently been clarified [18], the physics of their anomalously strong interaction with the light remains a mystery. This paper presents the experimental study of the electrodynamic response of a gated 2DES loaded by an external on-chip resonator. In this case, we observe a substantial reduction in the resonant plasma frequency and drastic narrowing of the plasma resonance caused by the hybridization of the 2D plasma with the light modes. Importantly, we develop a rigorous theory to expound on the coupling between the relativistic plasmon and the resonator. Our experimental results show good agreement with the theory.

The experiments were conducted on an $Al_{0.24}Ga_{0.76}As/GaAs/Al_{0.24}Ga_{0.76}As$ heterostructure hosting a two-dimensional electron system in a single 30 nm-wide quantum well located at a distance $h = 370$ nm below the crystal surface. The sample with two-dimensional electron density $n_s = 2.4 \times 10^{11}$ cm^{-2} and electron mobility $\mu = 2.5 \times 10^6$ cm^2/V s was measured at the temperature of 1.5 K. The sample structure was patterned after the Corbino geometry using optical lithography tools, as depicted in Fig. 1. The 2DES disk with diameter $D = 0.5$ mm was partially screened by the central gate of diameter $d = 0.1$ mm. The ohmic Au/Ge contact was formed around the perimeter of the 2DES. The gate and the contact were electrically connected through a meander-like external resonator circuit lithographically fabricated on the surface of the chip (Fig. 1). The values of circuit inductance L_m and capacitance C_m were determined by running a simulation in Ansys HFSS software and verified by the direct measurement with an RLC-meter. In our experiments, we used microwave radiation in the frequency range of 0.150 GHz. The signal was guided to the sample through a coaxial cable terminated in a wire antenna. To detect the plasma excitations, we employed a nondestructive optical technique [23]. It is based on the high sensitivity of the 2DES luminescence spectrum to the heating caused by the absorption of microwave radiation. The sample was placed into a cryostat with the base temperature of 1.5 K inside a superconducting coil producing the magnetic field B in the range of 0–0.6 T.

Figure 2(a) shows the microwave absorption versus the applied magnetic field. The data are obtained for the excitation frequencies of 3.6, 11.5, and 16.3 GHz. The sample
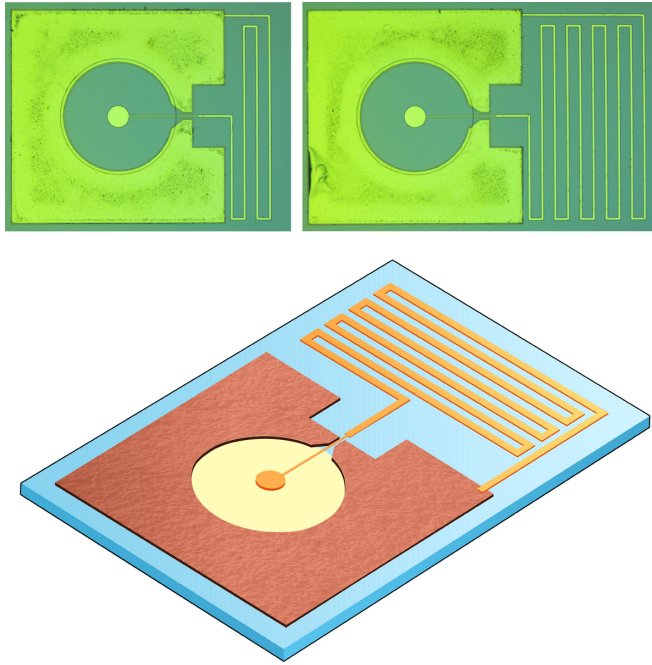
FIG. 1. Schematic drawing and photos of the experimental sample structure. The contact area, the 2DES, and the gate are shown in brown, yellow, and orange, respectively. A meander microstrip line plays the role of the external resonator.
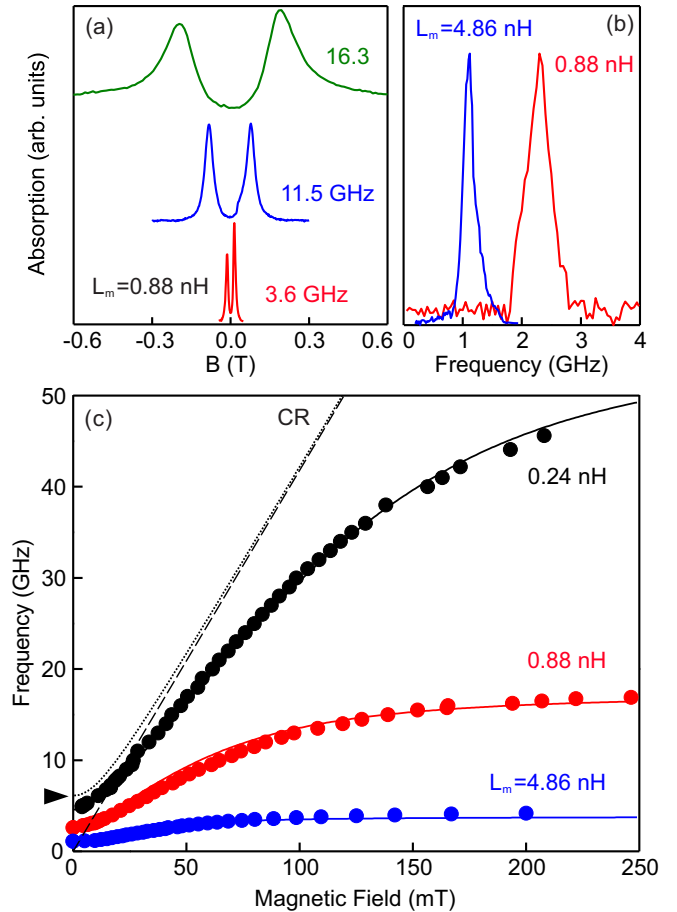

FIG. 2. (a) Dependence of the microwave absorption on the magnetic field measured at different frequencies. The sample has the gate diameter $d = 0.1$ mm, electron density $n_s = 2.4 \times 10^{11}$ cm^{-2}, and on-chip resonator circuit inductance $L_m = 0.88$ nH. The curves are offset vertically for clarity. (b) Microwave absorption spectra measured at $B = 0$ T for two geometrically identical samples with resonator inductances of 0.88 nH (red) and 4.86 nH (blue). (c) Comparison between magnetodispersions of the relativistic plasma mode measured for the same structural geometry but different resonator inductances of 0.24 nH (black dots), 0.88 nH (red dots), and 4.86 nH (blue dots). The dotted curve presents quasistatic prediction for the magnetodispersion $\omega_p = \sqrt{\omega_0^2 + \omega_c^2}$. The solid curves are the prediction of the developed theoretical model. The dashed line is the cyclotron resonance (CR) frequency $\omega_c = eB/m^*$.

under investigation includes an external resonant circuit of the inductance $L_m = 0.88$ nH and capacitance $C_m = 0.03$ pF, connected between the center gate and the outer perimetric contact (Fig. 1). We note that for all tested resonators, the value of C_m is negligible compared to the capacitance of the gated region of the 2DES, $C = 2.4$ pF. Hence, in what follows, we are interested only in the values of L_m. The curves in Fig. 2(a) clearly indicate the resonant peak that rapidly moves to larger magnetic fields with increasing excitation frequency. According to the previous studies [18], the observed resonance corresponds to the excitation of a relativistic plasmon—the low-frequency plasma mode that becomes dominant when the gate is electrically connected to the 2DES. In the case of a short-circuited gate and 2DES, the relativistic plasmon frequency can be expressed as [18]:

$$\omega_0 = \sqrt{\frac{2}{1/4 + \ln(D/d)}} \sqrt{\frac{n_s e^2 h}{m^* \varepsilon \varepsilon_0} \frac{2}{d}} \qquad (D/d > 2), \quad (1)$$

where e is the electron charge, n_s and m^* are the density and effective mass of the 2D electrons, ε_0 and ε are the permittivities in vacuum and dielectric, D and d are the diameters of the 2DES and the gate, and h is their separation distance.

In our experiments, we have tested eleven samples with different values of the resonator inductance. For each external resonator, we measured the resonant frequency as a function of the magnetic field. Figure 2(c) displays the magnetodispersions recorded for $L_m = 0.24, 0.88$, and 4.86 nH. The data indicate that the resonator causes substantial changes in the resonant frequency and the magnetic-field dependency of the relativistic plasmon. For example, the zero-field plasma frequency is drastically reduced compared to the quasistatic

value from Eq. (1) marked by the black arrow in the figure. For the resonator with $L_m = 4.86$ nH, it decreases more than fivefold, from $f_0 = 6.0$ GHz to $f_p = 1.1$ GHz [blue curve in Fig. 2(b)], where the reduction in frequency is accompanied by a significant narrowing of the plasma resonance line. At the same time, the magnetic-field behavior of the plasma mode undergoes considerable transformation due to its hybridization with the photonic mode of the resonator. The magnetodispersion crosses the CR line $\omega_c = eB/m^*$ [dashed line in Fig. 2(c)], while for high magnetic fields, the plasmon frequency asymptotically tends to that of the resonator photon mode [18]. The observed pattern is in stark contrast to the

quasistatic case with $\omega_p = \sqrt{\omega_0^2 + \omega_c^2}$, plotted in the dotted line in Fig. 2(c).

To substantiate such an abnormal behavior of the relativistic plasmon, we have developed a rigorous theory that takes into account the electrodynamics of the complex system under study [24]. However, the same results can be obtained quantitatively by an intuitive lumped-element approach [25–29]. Let us consider an axisymmetric plasma excitation in a 2DES disk with a radially directed electric field. The longitudinal of the 2DES conductivity tensor can be described by the Drude formula:

$$\sigma_s(\omega, B) = \frac{n_s e^2 \tau}{m^*} \frac{1 + i\omega\tau}{(1 + i\omega\tau)^2 + \omega_c^2\tau^2}, \quad (2)$$

where τ is the transport relaxation time. In this case, the 2DES impedance per square, $Z_s = 1/\sigma_s$, can be decomposed into the "lumped" element resistance and reactance. Hence, in the limit of $\omega\tau \gg 1$, the 2DES impedance can be factored out as

$$Z_s(\omega, B) = R_s + i\omega L_\square, \quad (3)$$

where $L_\square$ is the kinetic inductance of the 2DES and R_s is the resistance per square. The $L_\square$ results from the kinetic energy that electrons gain in an alternating electric field. From Eq. (2), it follows that

$$L_\square(\omega, B) = \frac{m^*}{n_s e^2}\left(1 - \frac{\omega_c^2}{\omega^2}\right). \quad (4)$$

It has been established that relativistic plasmons are charge oscillations between the gate and 2DES that involve the charge flow through the external circuit. Therefore, the relativistic mode can be regarded as a resonance in a series resonant circuit composed of the kinetic inductance of 2D electrons, L_k, an external circuit, and the capacitance between the center gate and the 2DES, C. If we assume the impedance of the external circuit to be negligible, the resonant plasmon frequency can be expressed as $\omega_0 = 1/\sqrt{L_k C}$, where the inductance and capacitance are defined by the structure geometry under study as follows: [24]

$$L_k = \frac{m^*}{2\pi n_s e^2}\left(\ln\left(\frac{D}{d}\right) + \frac{1}{4}\right), \quad C = \frac{\varepsilon\varepsilon_0 \pi d^2/4}{h}. \quad (5)$$

The effect of an external resonator can be taken into account by adding the microstrip magnetic inductance, L_m, as an extra term in the net inductance of the resonant LC circuit: $L = L_k(1 - \omega_c^2/\omega^2) + L_m$. Here, we also include the magnetic-field dependence of the 2DES kinetic inductance from Eq. (4). Since a typical external resonator capacitance (0.05 pF) is much less than the capacitance between the gate and 2DES (2.4 pF), the C_m term can be neglected at small magnetic fields when the resonant frequencies of the relativistic plasmon and the resonator are far apart.

$$\omega_p^2 = \frac{1}{LC} = \frac{\omega_0^2 + \omega_c^2}{1 + \frac{L_m}{L_k}}. \quad (6)$$

We note that the change in the plasma frequency ω_p due to the magnetic inductance L_m can be treated as the manifestation of electromagnetic retardation. It is usually quantified by introducing the dimensionless retardation parameter A—a measure of the plasmon-photon coupling [6,7]. In our case, given the Eq. (6), it is convenient to consider the retardation parameter in the form $A^2 = L_m/L_k$. Thus, the plasmon frequency and the effective CR frequency are scaled by a factor $1/\sqrt{1 + A^2}$, reflecting the extent of plasmon-photon hybridization. This concept has a wide range of applications. For example, the same approach can be used to account for the retardation effects of ordinary plasmons in gated and ungated 2DESs [24].

To validate the proposed notion of relativistic plasmon-photon coupling, we conducted a series of experiments on a set of structures with different on-chip resonators. For these measurements, all the samples had the same 2DES parameters—a fixed kinetic inductance $L_k = 0.29$ nH according to (5). For the resonator circuit, we used a meander microstrip line with a different number of sections (Fig. 1). The magnetic inductance L_m was calculated numerically using CST Microwave Studio and verified by direct measurements with RLC-meter (see Supplemental Material [24] for more details). As a result, we obtained the values of magnetic inductance in the range of 0.88–9.1 nH.

Figure 3 shows the relativistic plasmon frequency ω_p/ω_0 and the effective CR frequency ω_c'/ω_c as a function of the retardation parameter A. In the figure, we compare the experimental data, plotted in red and blue circles, with the theoretical dependency $1/\sqrt{1 + A^2}$ according to Eq. (6), denoted with respective solid curves. These results indicate good agreement between the theory and experiment. As for the estimate of ω_c', we note that in the limit of small magnetic fields, the magnetodispersions from Fig. 2 are well approximated by the quadratic dependence on B, as illustrated by the inset to Fig. 3(b). Here, the magnetodispersion for the 0.88 nH resonator is plotted as f^2 versus B^2. Hence, the effective CR frequency ω_c' can be determined using the linear fit of the experimental data at $B = 0$ T.

Notably, the dependencies in Fig. 3 are qualitatively similar to those obtained for the ordinary plasmon-polariton modes excited in a disk and stripe geometries [6,30]. However, the magnitude of the 2D plasma hybridization with light far exceeds the level expected in the case of ordinary 2D plasmons indicated by the dashed line in Fig. 3(a). Such an ultrastrong hybridization of the relativistic plasmon with light ultimately leads to extremely weak damping of the plasmonic mode [16,17]. It is also worth noting that the beauty of data representation in Fig. 3 is that both dependencies are expressed in a dimensionless form. As a result, the measurement of samples with arbitrary parameters and resonator dimensions can be reduced to a single universal dependence.

Another significant implication of the developed model is that it explains why hybridization between the relativistic plasmon and light leads to a drastic decrease in the plasmon damping. According to the theory [24], at zero magnetic field, the half-width of the relativistic plasmon resonance can be
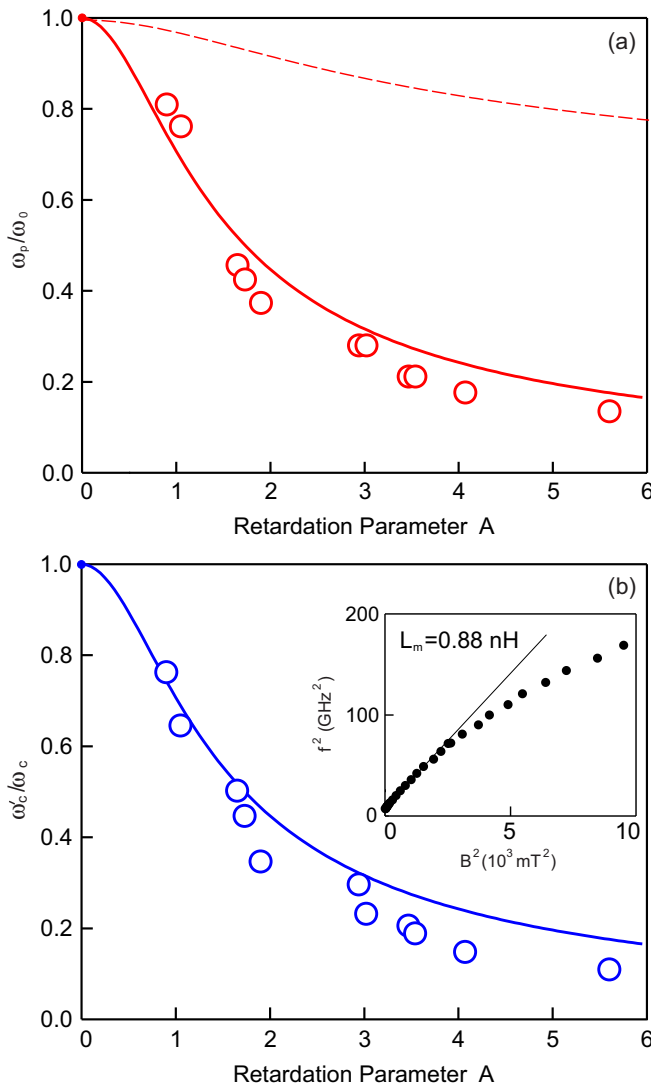
FIG. 3. The normalized resonant frequency of the relativistic plasmon at zero magnetic field (a) and the normalized effective CR frequency (b), plotted versus the retardation parameter A. In both pictures, the experimental data (red and blue circles) are compared to the theoretical dependency $1/\sqrt{1 + A^2}$ (solid lines) based on equation (6). The dashed line represents the prediction for ordinary plasmon-polariton modes [6,30]. The inset illustrates the comparison between the measurement data for the 0.88 nH resonator (black dots), plotted as frequency squared versus the square of the magnetic field, and the linear behavior in the limit of low magnetic fields (solid black line).

written as

$$\Delta\omega = \frac{1}{\tau}\frac{1}{1 + A^2}. \qquad (7)$$

In essence, the plasmon damping is suppressed due to the delocalization of the plasma mode from a lossy 2DES to the external resonator. In this case, it is of particular interest to estimate the Q-factor of the relativistic plasmon in the limit of strong retardation:

$$\frac{\omega_p}{2\Delta\omega} = \frac{\omega_0\tau}{2}\sqrt{1 + A^2}$$

$$\approx \frac{\sigma_0}{c\,\varepsilon_0} \times \sqrt{\frac{hL_m}{d^2\mu_0}}$$

$$\times \frac{1}{\ln(D/d) + 1/4}\frac{2\sqrt{\pi}}{\sqrt{\varepsilon}}, \qquad (8)$$

where $\sigma_0 = n_s e^2 \tau/m^*$ is a static conductivity of the 2DES at zero magnetic field and c is the speed of light in vacuum. Here, the quotient $\frac{L_m}{\mu_0}$ can be understood as an effective length of the external resonator, corresponding to its magnetic inductance. Indeed, for the external resonator with $L_m = 0.88$ nH, the experimental data from Fig. 2(b) yields $Q = 4.7$. This value is relatively consistent with the prediction of $Q = 6.2$ calculated from equation (8). Remarkably, we observe the relativistic plasma mode in the frequency range $\omega_p\tau < 1$, where the ordinary plasmons are overdamped. For example, for the resonator with $L_m = 4.86$ nH, the resonance plotted in blue color in Fig. 2(b) occurs at $\omega_p\tau = 0.66$.

In conclusion, we have experimentally investigated the relativistic plasma excitation in a partly screened two-dimensional electron system loaded by an external on-chip resonator. We have observed that the relativistic plasmon strongly couples to the resonator photon mode, causing a drastic reduction in the plasma frequency and linewidth. We have developed a physical approach that accurately describes the ultrastrong hybridization of 2D plasma with light. The predictions of the proposed model show good agreement with the experimental data. Furthermore, it has been found that in the regime of strong retardation, the damping of the relativistic plasmon is determined by the parameter $\sigma_0/c\,\varepsilon_0$.

[1] J. J. Hopfield, Phys. Rev. **112**, 1555 (1958).

[2] D. N. Basov, M. M. Fogler, and F. J. García de Abajo, Science **354**, aag1992 (2016).

[3] D. A. Iranzo, S. Nanot, F. J. C. Dias *et al.*, Science **360**, 291 (2018).

[4] I. Epstein, D. Alcaraz, Z. Huang *et al.*, Science **368**, 1219 (2020).

[5] W. L. Barnes, A. Dereux, and T. W. Ebbesen, Nature (London) **424**, 824 (2003).

[6] I. V. Kukushkin, J. H. Smet, S. A. Mikhailov, D. V. Kulakovskii, K. von Klitzing, and W. Wegscheider, Phys. Rev. Lett. **90**, 156801 (2003).

[7] S. A. Mikhailov and N. A. Savostianova, Phys. Rev. B **71**, 035320 (2005).

[8] I. V. Andreev, V. M. Muravev, N. D. Semenov, and I. V. Kukushkin, Phys. Rev. B **103**, 115420 (2021).

[9] D. Heitmann, Surf. Sci. **170**, 332 (1986).

[10] F. H. Koppens, D. E. Chang, and F. J. Garcia de Abajo, Nano Lett. **11**, 3370 (2011).

[11] G. Scalari, C. Maissen, D. Turcinkova, D. Hagenmüller, S. De Liberato, C. Ciuti, C. Reichl, D. Schuh, W. Wegscheider, M. Beck, and J. Faist, Science **335**, 1323 (2012).

[12] Q. Zhang, T. Arikawa, E. Kato, J. L. Reno, W. Pan, J. D. Watson, M. J. Manfra, M. A. Zudov, M. Tokman, M. Erukhimova, A. Belyanin, and J. Kono, Phys. Rev. Lett. **113**, 047601 (2014).

[13] J. Lusakowski, Semicond. Sci. Technol. **32**, 013004 (2017).

[14] D. A. Bandurin, D. Svintsov, I. Gayduchenko, S. G. Xu, A. Principi, M. Moskotin, I. Tretyakov, D. Yagodkin, S. Zhukov, T. Taniguchi, K. Watanabe, I. V. Grigorieva, M. Polini, G. N. Goltsman, A. K. Geim, and G. Fedorov, Nat. Commun. **9**, 5392 (2018).

[15] P. Forn-Díaz, L. Lamata, E. Rico, J. Kono, and E. Solano, Rev. Mod. Phys. **91**, 025005 (2019).

[16] P. A. Gusikhin, V. M. Muravev, and I. V. Kukushkin, JETP Lett. **100**, 648 (2015).

[17] V. M. Muravev, P. A. Gusikhin, I. V. Andreev, and I. V. Kukushkin, Phys. Rev. Lett. **114**, 106805 (2015).

[18] V. M. Muravev, P. A. Gusikhin, A. M. Zarezin, A. A. Zabolotnykh, V. A. Volkov, and I. V. Kukushkin, Phys. Rev. B **102**, 081301(R) (2020).

[19] A. A. Zabolotnykh and V. A. Volkov, Phys. Rev. B **99**, 165304 (2019).

[20] V. M. Muravev, P. A. Gusikhin, A. M. Zarezin, I. V. Andreev, S. I. Gubarev, and I. V. Kukushkin, Phys. Rev. B **99**, 241406(R) (2019).

[21] A. M. Zarezin, P. A. Gusikhin, V. M. Muravev, and I. V. Kukushkin, JETP Lett. **111**, 282 (2020).

[22] A. M. Zarezin, P. A. Gusikhin, I. V. Andreev, V. M. Muravev, and I. V. Kukushkin, JETP Lett. **113**, 713 (2021).

[23] I. V. Kukushkin, J. H. Smet, K. von Klitzing, and W. Wegscheider, Nature (London) **415**, 409 (2002).

[24] See Supplemental Material at http://link.aps.org/supplemental/10.1103/PhysRevB.105.L041403 for theoretical treatment of the relativistic plasma excitation, external resonators magnetic inductance calculation, and retardation parameter consideration.

[25] P. J. Burke, I. B. Spielman, J. P. Eisenstein, L. N. Pfeiffer, and K. W. West, Appl. Phys. Lett. **76**, 745 (2000).

[26] G. R. Aizin and G. C. Dyer, Phys. Rev. B **86**, 235316 (2012).

[27] H. Yoon, K. Y. M. Yeung, V. Umansky, and D. Ham, Nature (London) **488**, 65 (2012).

[28] G. C. Dyer, G. R. Aizin, S. J. Allen, A. D. Grine, D. Bethke, J. L. Reno, and E. A. Shaner, Nat. Photonics **7**, 925 (2013).

[29] V. M. Muravev, N. D. Semenov, I. V. Andreev, P. A. Gusikhin, and I. V. Kukushkin, Appl. Phys. Lett. **117**, 151103 (2020).

[30] I. V. Kukushkin, V. M. Muravev, J. H. Smet, M. Hauser, W. Dietsche, and K. von Klitzing, Phys. Rev. B **73**, 113310 (2006).